Publ. Astron. Soc. Japan (2016) 68 (3), 31 (1–12)
doi: 10.1093/pasj/psw023
Advance Access Publication Date: 2016 March 17

A precontact binary and a shallow contact binary are in the same field

Liang Liu,[1,2,3,*] Shengbang Qian,[1,2,3] Jiajia He,[1,2] Wenping Liao,[1,2] and Nianping Liu[1,2]

[1]Yunnan Observatories, Chinese Academy of Sciences (CAS), PO Box 110, 650011 Kunming, P.R. China
[2]Key Laboratory for the Structure and Evolution of Celestial Objects, Chinese Academy of Sciences, 650011 Kunming, P.R. China
[3]University of the Chinese Academy of Sciences, Yuquan Road 19#, Sijingshang Block, 100049 Beijing, P.R. China

* E-mail: LiuL@ynao.ac.cn

Received 2015 December 9; Accepted 2016 February 13

Abstract

The period changes of two close binaries, V1107 Cas and AX Cas, which are in the same field, were investigated. Their periods both show a long-term decrease. After further analysis, we found that the periods have their respective cyclic oscillations ($T_3 = 6.74 \pm 0.24$ yr for V1107 Cas and $T_3 = 13.8 \pm 0.3$ yr for AX Cas), which are possibly caused by a third body due to the light-time effect. We also obtained the complete VR_cI_c light curves for V1107 Cas and analyzed them with the 2010 version of the Wilson–Devinney code. The photometric results reveal that V1107 Cas is a W-type shallow contact (15.2%$\pm$1.8%) binary, with a mass-ratio of 1.797 ± 0.006. The period variation and photometric solution suggest that V1107 Cas is a newly formed contact binary system. Moreover, we estimated the fundamental parameters for V1107 Cas. They are: $M_1 = 0.39 \pm 0.01\,M_\odot$, $M_2 = 0.70 \pm 0.03\,M_\odot$, $R_1 = 0.52 \pm 0.10\,R_\odot$, $R_2 = 0.68 \pm 0.12\,R_\odot$, $L_1 = 0.178 \pm 0.108\,L_\odot$, and $L_2 = 0.196 \pm 0.116\,L_\odot$. Then, based on the coplane assumption, we deduced the masses of possible third bodies to be $M_3 = 0.091 \pm 0.019\,M_\odot$ for V1107 Cas and $M_3 = 0.325 \pm 0.029\,M_\odot$ for AX Cas. Finally, we inferred the evolutional stage of AX Cas, and believe that it is a precontact binary. Thus, the precontact binary AX Cas and the shallow contact binary V1107 Cas have adjoining evolutional stages.

Key words: binaries: close — binaries: eclipsing — stars: evolution — stars: individuals (V1107 Cassiopeiae; AX Cassiopeiae)

1 Introduction

Mass transfer is a common and very important process for close binaries, which drives the evolution of the systems, and had been used to explain the famous Algol paradox, as well many other interesting astrophysical processes. Understanding the mass transfer that occurs in near contact binaries or in marginal contact binaries is key to understanding how a semi-detached binary evolves into a contact binary (i.e., BL And and GW Tau, Zhu & Qian 2006; AS Ser, Zhu et al. 2008; DD Com, Zhu et al. 2010). Some such mass-transfer processes were affected by third bodies or by magnetic activeties (i.e., ZZ Eri, D. R. Faulkner et al. 2014;[1] GSC 1537−1557, AH Tau, and V508 Oph, Xiang et al. 2015a, 2015b, 2015c). The absolute physical parameters

[1] Faulkner, D. R., Clark, J., Samec, R. G., Hill, R. L., Kring, J., Flaaten, D., & Van Hamme, W. V. 2014, Abstract, AAS Meeting #223, id.155.11.

that combine the orbital elements are a great help for digging out evolutionary information concerning a close binary, so we monitored the times of the minima for V1107 Cas, and observed its multiple color light curves, while intending to find the evolutional stage of V1107 Cas. During the data processing, we realized that the other close binary, AX Cas, had been observed in the same field, by chance. AX Cas had not been included in our observational schedule because it is not an EW but EB-type binary. However, after having investigated some of the literature (i.e., AK CMi, Samec et al. 1998; V2421 Cyg, Samec et al. 2014), we became aware that AX Cas may be a precontact binary. It is very interesting that a precontact and a contact binary are in the same field.

Until and after V1107 Cas (GSC 04030−02020) had been found as a W UMa variable (Hoffman et al. 2009), there were only 10 papers written about it; none of them as an individual study. From the 2 Micron All-Sky Survey (2MASS) catalogue (R. M. Cutri et al. 2003),[2] we found its *JHK* magnitudes to be $J = 11.250 \pm 0.023$, $H = 10.806 \pm 0.024$, and $K = 10.717 \pm 0.018$. And according to the NOMAD Catalog (N. Zacharias et al. 2005),[3] we found its *BVR* magnitudes to be $B = 13.790$, $V = 13.310$, and $R = 12.770$. The yielded color indexes by these magnitudes were used to estimate the effective temperature of star 1 in our photometric solution. As for the other close binary, AX Cas, it was discovered as early as 1931 by Beljawsky (1931). We found its *JHK* magnitudes to be $J = 10.991 \pm 0.022$, $H = 10.655 \pm 0.019$, and $K = 10.532 \pm 0.016$ (R. M. Cutri et al. 2003), 2 and its *BVR* magnitudes to be $B = 13.010$, $V = 12.640$, and $R = 12.180$ (N. Zacharias et al. 2005).[3] We computed the masses, radii, and absolute thermal magnitudes of its components as $M_1 = 2.0\,M_\odot$, $M_2 = 0.45\,M_\odot$, $R_1 = 2.10\,R_\odot$, $R_2 = 1.00\,R_\odot$, $M_{\rm bol1} = 1.35$ mag, $M_{\rm bol2} = 4.80$ mag (M. A. Svechnikov & Eh. F. Kuznetsova 1990).[4] However, the color indexes did not agree with the less-massive component. We discuss this in section 5.

2 New CCD imaging photometry

We obtained complete VR_cI_c light curves of V1107 Cas on 2013 August 18 and 25, using the 1024 × 1024 PI1024 BFT camera attached to the 85 cm telescope at the Xinglong Station of the National Astronomical Observatories of the Chinese Academy of Sciences. The observational system has a standard Johnson–Cousins–Bessel multicolor CCD photometric system built on the primary focus (Zhou et al. 2009), generating an effective field of view equal to $16\farcm5 \times 16\farcm5$. We also obtained several times of minima of V1107 Cas, using the DW436 2048 × 2048 CCD photometric system attached to the 1 m reflecting telescope and the DV436 2048 × 2048 CCD photometric system attached to the 60 cm reflecting telescope at the Yunnan Observatories (YNOs) in China. Both filter systems were the Johnson–Cousins–Bessel system. The effective field of view of the 1 m telescope was $7\farcm3 \times 7\farcm3$, while that of the 60 cm telescope was $12' \times 12'$ at the Cassegrain focus. These times of minima of V1107 Cas are listed in table 1, where "1 m" and "60 cm" refer to the times of minima monitored with the 1 m and 60 cm telescopes at the YNOs, respectively; "85 cm" refers to those monitored with the 85 cm telescope at the Xinglong Station. 2MASS J01233287+6135269 (star 1) and 2MASS J01232239+6131552 (star 2) were used for photometric comparisons. The PHOT/IRAF aperture photometry package was exercised so as to reduce the images, using the standard procedure of flat-fielding, except for dark corrections, because the dark value of the images was very insignificant. The corresponding light curves of V1107 Cas are shown in figure 1, where the phases were calculated with equation (6). On the other hand, the light levels of the curves taken on two nights match very well, suggesting little nightly variation. On the other hand, the magnitude differences between the two comparison stars remained nearly constant, vindicating the assumption that the comparisons are nonvariable. A quadratic polynomial model was used to determine the times of minima for V1107 Cas by the least-squares method. Our new times of minima are listed in table 1. Because the other close binary AX Cas is close to V1107 Cas in visual, it was observed at the same time in most of our frames. Although we did not obtain complete light curves of AX Cas, we obtained some times of minima. They are also listed in table 1.

3 Photometric solutions of V1107 Cas

Multicolor light curves of V1107 Cas were analyzed with the 2010 Version of the Wilson–Devinney (W–D) code (Wilson & Devinney 1971; Wilson 1979, 1990, 1994, 2008; Van Hamme & Wilson 2007). The effective temperature of star 1 was estimated from the colors of V1107 Cas mentioned in section 1 using the program of Worthey and Lee (2011). It should range between 4900 K and 5500 K. In the solution, we took the temperature as 5200 K, and then used the temperature range to limit its uncertainty.

[2] Cutri, R. M., et al. 2003, 2MASS All-Sky Catalog of Point Sources, VizieR Online Data Catalog, II/246 ⟨http://cdsarc.u-strasbg.fr/viz-bin/Cat?II/246⟩.

[3] Zacharias, N., Monet, D. G., Levine, S. E., Urban, S. E., Gaume, R., & Wycoff, G. L. Naval Observatory Merged Astrometric Dataset (NOMAD), VizieR Online Data Catalog, I/297 ⟨http://cdsarc.u-strasbg.fr/viz-bin/Cat?I/297⟩.

[4] Svechnikov, M. A., & Kuznetsova Eh. F. 1990, Catalogue of approximate photometric and absolute elements of eclipsing variable stars ⟨http://cdsarc.u-strasbg.fr/viz-bin/Cat?V/124⟩.

Table 1. New times of light minimum for AX Cas and V1107 Cas.

JD (Hel.) (d)	Error (d)	Min.	Filter	Telescope
		—AX Cas—		
2456214.22009	0.00011	sec.	No	1 m
2456220.22436	0.00038	sec.	V	1 m
2456220.22450	0.00034	prim.	R_c	1 m
2456220.22467	0.00033	prim.	I_c	1 m
2456220.22476	0.00041	sec.	B	1 m
		—V1107 Cas—		
2456209.16515	0.00011	sec.	No	60 cm
2456214.21991	0.00012	prim.	No	1 m
2456220.23732	0.00021	prim.	V	1 m
2456220.23741	0.00020	prim.	R_c	1 m
2456220.23753	0.00019	prim.	I_c	1 m
2456220.23755	0.00025	prim.	B	1 m
2456220.37551	0.00045	sec.	B	1 m
2456220.37568	0.00026	sec.	R_c	1 m
2456220.37570	0.00031	sec.	V	1 m
2456220.37583	0.00029	sec.	I_c	1 m
2456523.31517	0.00015	sec.	I_c	85 cm
2456523.31517	0.00011	sec.	V	85 cm
2456523.31522	0.00013	sec.	R_c	85 cm
2456530.28646	0.00009	prim.	I_c	85 cm
2456530.28673	0.00009	prim.	V	85 cm
2456530.28691	0.00008	prim.	R_c	85 cm

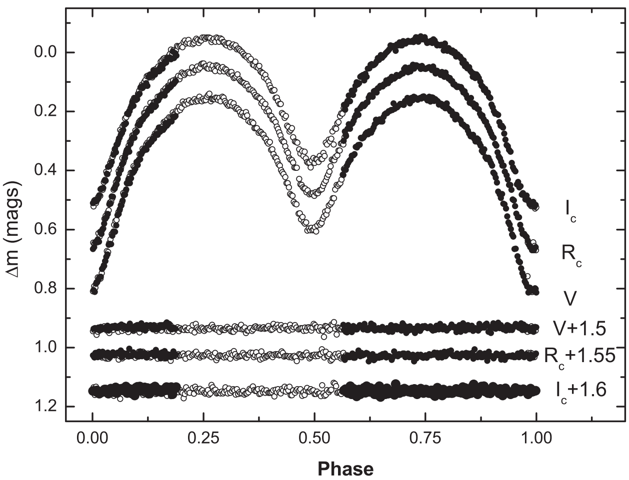

Fig. 1. VR_cI_c-band light curves of V1107 Cas taken on 2012 August 18 and 25. The light levels of the curves taken on the two nights match very well, suggesting little nightly variation. The two-day light curves are phased up smoothly, suggesting little nightly fluctuations.

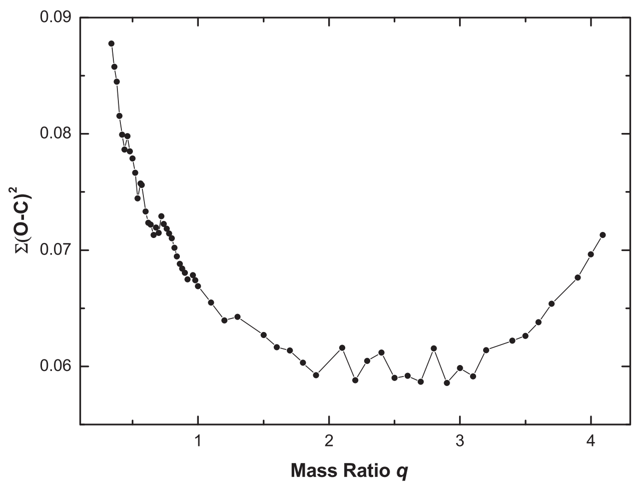

Fig. 2. Relationship between the mass ratio, q, the fitting residual.

We thus have $T_1 = 5200 \pm 300\,\mathrm{K}$. We then used the q-search method to obtain an initial input value of the mass ratio, q. The details are: we fixed the mass ratio q at a series of values of 0.1, 0.2, 0.3, etc.; we then fitted the light curves with the W–D code for each q value, obtaining a series of corresponding fitting residuals, illustrated in figure 2, and selected the final q value with minimal residuals. The mass ratio should thus be between 1.6 and 3.2. While obtaining the solution, the bolometric albedo $A_1 = A_2 = 0.5$ (Rucinski 1969) and the values of the gravity-darkening coefficient $g_1 = g_2 = 0.32$ (Lucy 1967) were used, which correspond to the common convective envelope of both components. According to Claret and Gimenez (1990), the square-root limb-darkening coefficients were used. We adjusted the mass ratio, q; the mean temperature of star 2, T_2; the monochromatic luminosity of star 1 and the dimensionless

Table 2. Photometric solutions for V1107 Cas.

Parameters	Without l_3 VR_cI_c	Errors	With l_3 VR_cI_c	Errors
$g_1 = g_2$	0.32	fixed	0.32	fixed
$A_1 = A_2$	0.50	fixed	0.50	fixed
$x_{1bolo} = x_{2bolo}, y_{1bolo} = y_{2bolo}$	0.271, 0.433	fixed	0.271, 0.433	fixed
$x_{1V} = x_{2V}, y_{1V} = y_{2V}$	0.468, 0.373	fixed	0.468, 0.373	fixed
$x_{1R_c} = x_{2R_c}, y_{1R_c} = y_{2R_c}$	0.307, 0.483	fixed	0.307, 0.483	fixed
$x_{1I_c} = x_{2I_c}, y_{1I_c} = y_{2I_c}$	0.199, 0.508	fixed	0.199, 0.508	fixed
T_1(K)	5200	±300,fixed	5200	±300,fixed
T_2(K)	4657	±306	4657	±306
$q = M_2/M_1$	1.808	±0.005	1.797	±0.006
i (°)	72.0	±0.1	72.3	±0.5
$\Omega_1 = \Omega_2$	4.8898	±0.0095	4.8721	±0.0106
Ω_{in}	4.9773	—	4.9615	—
Ω_{out}	4.3866	—	4.3713	—
$L_1/(L_1 + L_2)(V)$	0.5252	±0.0020	0.5266	±0.0114
$L_1/(L_1 + L_2)(R_c)$	0.4945	±0.0016	0.4959	±0.0106
$L_1/(L_1 + L_2)(I_c)$	0.4757	±0.0013	0.4772	±0.0102
$l_3/(L_1 + L_2 + l_3)(V)$	—	—	0.0011	±0.0114
$l_3/(L_1 + L_2 + l_3)(R_c)$	—	—	0.0006	±0.0106
$l_3/(L_1 + L_2 + l_3)(I_c)$	—	—	0.0016	±0.0102
r_1 (pole)	0.3159	±0.0010	0.3166	±0.0012
r_1 (side)	0.3312	±0.0012	0.3319	±0.0014
r_1 (back)	0.3688	±0.0020	0.3697	±0.0023
r_2 (pole)	0.4137	±0.0009	0.4134	±0.0010
r_2 (side)	0.4402	±0.0012	0.4399	±0.0013
r_2 (back)	0.4721	±0.0016	0.4719	±0.0018
f (%)	14.8	±1.6	15.2	±1.8

potential of star 1. We started the differential corrections (DC) program at model 2. After thousands of iterations, it converged to model 3 ($\Omega_1 = \Omega_2$, mode 3 for contact configuration). The photometric solution is listed in table 2 and the theoretical light curves computed with those photometric elements are plotted in figure 3. We also ran the program with l_3 light, because the period investigation of V1107 Cas, described in next section, implied that it has a third companion. The outcomes (table 2) showed that the third companion has no more than a 0.16% luminosity contribution to the whole system. Its details are given in section 5.

According to the photometric solution, we concluded that V1107 Cas is a moderate mass-ratio (1.797 ± 0.006), shallow contact (15.2%±1.8%) binary, where "shallow" is defined when the contact degree is less than 20%. We assumed that primary component of V1107 Cas is a normal main-sequence star. Accordingly, we found its temperature to be $T = 4657 \pm 306$ K, and estimated its mass at $M = 0.70 \pm 0.03$. We then estimated the physical parameters of each component by using of the light-curve (LC) program, W–D code (Wilson & Devinney 1971; Wilson 1979, 1990, 1994, 2008; Van Hamme & Wilson 2007). The results are

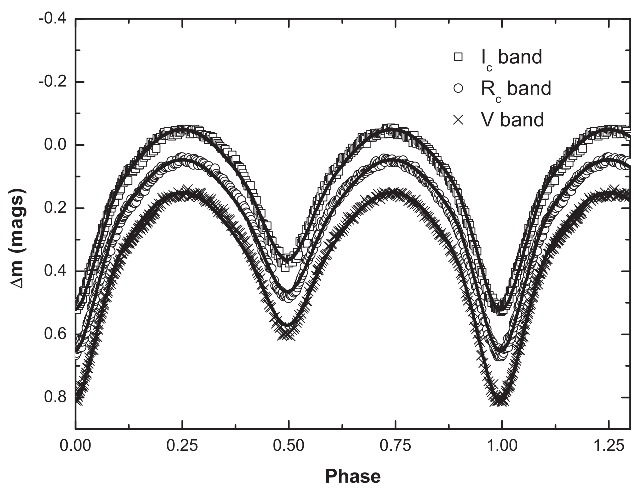

Fig. 3. Observed and theoretical light curves in the V, R_c, and I_c bands of V1107 Cas, with l_3 light.

$M_1 = 0.39 \pm 0.01\, M_\odot$, $M_2 = 0.70 \pm 0.03\, M_\odot$, $R_1 = 0.52 \pm 0.10\, R_\odot$, $R_2 = 0.68 \pm 0.12\, R_\odot$, $L_1 = 0.178 \pm 0.108\, L_\odot$, and $L_2 = 0.196 \pm 0.116\, L_\odot$. The estimated uncertainties of the absolute parameters mainly result from the uncertainties of the temperatures of the components.

Table 3. CCD Times of light minima for V1107 Cas.

JD (Hel.)	Filters	Min.	Epoch	$(O-C)$ (d)	$(O-C)_1$ (d)	Residual (d)	Reference
2453215.4410		prim.	−12124	−0.00304	−0.00062	−0.00058	IBVS No. 5731
2453215.5786		sec.	−12123.5	−0.00214	0.00027	0.00031	IBVS No. 5731
2453254.4031		sec.	−11981.5	−0.00211	0.00018	0.00038	IBVS No. 5731
2453637.4522		sec.	−10580.5	−0.00290	−0.00165	−0.00020	IBVS No. 5731
2454085.3015		sec.	−8942.5	−0.00208	−0.00176	−0.00050	IBVS No. 5761
2454092.2753		prim.	−8917	−0.00028	0.00001	0.00126	IBVS No. 5874
2454092.4111		sec.	−8916.5	−0.00118	−0.00088	0.00036	IBVS No. 5874
2454092.5478		prim.	−8916	−0.00119	−0.00089	0.00035	IBVS No. 5874
2454092.6810		sec.	−8915.5	−0.00469	−0.00439	−0.00315	IBVS No. 5874
2454308.4086		sec.	−8126.5	0.00102	0.00097	0.00149	IBVS No. 5874
2454367.3284		prim.	−7911	0.00058	0.00045	0.00074	IBVS No. 5874
2454367.4657		sec.	−7910.5	0.00118	0.00105	0.00133	IBVS No. 5874
2454367.6015		prim.	−7910	0.00027	0.00014	0.00042	IBVS No. 5874
2454388.3799		prim.	−7834	−0.00062	−0.00077	−0.00057	IBVS No. 5874
2454388.5175		sec.	−7833.5	0.00027	0.00011	0.00031	IBVS No. 5874
2454388.6539		prim.	−7833	−0.00003	−0.00018	0.00000	IBVS No. 5874
2454390.2941		prim.	−7827	−0.00030	−0.00046	−0.00027	IBVS No. 6070
2454673.5509		prim.	−6791	0.00190	0.00143	0.00051	IBVS No. 5918
2454704.8561		sec.	−6676.5	0.00146	0.00096	−0.00006	IBVS No. 5875
2454776.3525		prim.	−6415	0.00068	0.00013	−0.00110	IBVS No. 5918
2454776.4901		sec.	−6414.5	0.00157	0.00102	−0.00021	IBVS No. 5918
2454835.2734		sec.	−6199.5	0.00134	0.00075	−0.00062	IBVS No. 5918
2454847.3039		sec.	−6155.5	0.00173	0.00113	−0.00027	IBVS No. 5918
2454847.4412		prim.	−6155	0.00232	0.00172	0.00031	IBVS No. 5918
2454847.5771		sec.	−6154.5	0.00151	0.00092	−0.00048	IBVS No. 5918
2455081.3444		sec.	−5299.5	0.00175	0.00106	−0.00055	IBVS No. 5941
2455081.4805		prim.	−5299	0.00115	0.00045	−0.00116	IBVS No. 5941
2455081.6183		sec.	−5298.5	0.00224	0.00154	−0.00007	IBVS No. 5941
2455154.3459		sec.	−5032.5	0.00231	0.00160	0.00003	IBVS No. 5941
2455154.4840		prim.	−5032	0.00370	0.00299	0.00143	IBVS No. 5941
2455154.6182		sec.	−5031.5	0.00120	0.00049	−0.00107	IBVS No. 5941
2455374.4429		sec.	−4227.5	0.00284	0.00213	0.00103	IBVS No. 5984
2455409.4380		sec.	−4099.5	0.00123	0.00054	−0.00045	IBVS No. 5984
2455479.2941		prim.	−3844	0.00062	−0.00004	−0.00079	IBVS No. 5984
2455479.4324		sec.	−3843.5	0.00222	0.00154	0.00080	IBVS No. 5984
2455479.5689		prim.	−3843	0.00201	0.00134	0.00059	IBVS No. 5984
2455482.3017	*R*	prim.	−3833	0.00069	0.00002	−0.00070	B.R.N.O. No.37
2455482.4394	*R*	sec.	−3832.5	0.00169	0.00102	0.00028	B.R.N.O. No.37
2455491.3259		prim.	−3800	0.00231	0.00164	0.00093	IBVS No. 5984
2455491.4624		sec.	−3799.5	0.00210	0.00143	0.00073	IBVS No. 5984
2455491.5976		prim.	−3799	0.00059	−0.00006	−0.00077	IBVS No. 5984
2455514.4290		sec.	−3715.5	0.00211	0.00145	0.00084	IBVS No. 5984
2455514.5662		prim.	−3715	0.00260	0.00195	0.00133	IBVS No. 5984
2455792.3489	*R*	prim.	−2699	−0.00105	−0.00153	−0.00101	B.R.N.O. No.38
2455792.4862	*R*	sec.	−2698.5	−0.00046	−0.00093	−0.00042	B.R.N.O. No.38
2455794.4008	*R*	sec.	−2691.5	0.00026	−0.00021	0.00030	B.R.N.O. No.38
2455794.5370	*R*	prim.	−2691	−0.00025	−0.00072	−0.00020	B.R.N.O. No.38
2455796.4504	*R*	prim.	−2684	−0.00073	−0.00120	−0.00067	B.R.N.O. No.38
2455796.5871	*R*	sec.	−2683.5	−0.00073	−0.00120	−0.00068	B.R.N.O. No.38
2455797.4080	*R*	sec.	−2680.5	−0.00007	−0.00054	−0.00001	B.R.N.O. No.38
2455797.5435	*R*	prim.	−2680	−0.00128	−0.00175	−0.00121	B.R.N.O. No.38
2455799.3220	*R*	sec.	−2673.5	0.00005	−0.00042	0.00011	B.R.N.O. No.38
2455799.4579	*R*	prim.	−2673	−0.00076	−0.00123	−0.00069	B.R.N.O. No.38
2455799.5947	*R*	sec.	−2672.5	−0.00066	−0.00113	−0.00059	B.R.N.O. No.38
2455802.3292	*R*	sec.	−2662.5	−0.00028	−0.00075	−0.00020	B.R.N.O. No.38

Table 3 (Continued)

JD (Hel.)	Filters	Min.	Epoch	$(O-C)$ (d)	$(O-C)_1$ (d)	Residual (d)	Reference
2455802.4650	R	prim.	−2662	−0.00119	−0.00165	−0.00110	B.R.N.O. No.38
2455805.3369	R	sec.	−2651.5	−0.00011	−0.00057	−0.00001	B.R.N.O. No.38
2455805.4725	R	prim.	−2651	−0.00122	−0.00168	−0.00112	B.R.N.O. No.38
2455805.6098	R	sec.	−2650.5	−0.00062	−0.00109	−0.00052	B.R.N.O. No.38
2455815.3159	R	prim.	−2615	−0.00064	−0.00109	−0.00049	B.R.N.O. No.38
2455815.4536	R	sec.	−2614.5	0.00035	−0.00010	0.00049	B.R.N.O. No.38
2455830.3531	R	prim.	−2560	−0.00109	−0.00153	−0.00087	B.R.N.O. No.38
2455830.4924	R	sec.	−2559.5	0.00151	0.00106	0.00172	B.R.N.O. No.38
2455831.3118	R	sec.	−2556.5	0.00067	0.00022	0.00088	B.R.N.O. No.38
2455831.4473	R	prim.	−2556	−0.00053	−0.00097	−0.00031	B.R.N.O. No.38
2455835.4135		sec.	−2541.5	0.00119	0.00075	0.00143	IBVS No. 6070
2455838.2831	R	prim.	−2531	−0.00003	−0.00046	0.00022	B.R.N.O. No.38
2455838.4203	R	sec.	−2530.5	0.00047	0.00002	0.00071	B.R.N.O. No.38
2455852.2271	R	prim.	−2480	−0.00003	−0.00045	0.00028	B.R.N.O. No.38
2455858.2432		prim.	−2458	0.00101	0.00059	0.00135	IBVS No. 6026
2455858.3804		sec.	−2457.5	0.00151	0.00108	0.00184	IBVS No. 6026
2455858.5156		prim.	−2457	0.00000	−0.00042	0.00034	IBVS No. 6026
2455875.3307	R	sec.	−2395.5	0.00028	−0.00012	0.00069	B.R.N.O. No.38
2455893.2382		prim.	−2330	−0.00069	−0.00108	−0.00019	IBVS No. 6026
2455905.6777		sec.	−2284.5	−0.00143	−0.00180	−0.00087	IBVS No. 6011
2456154.3465	R	prim.	−1375	−0.00063	−0.00070	0.00083	B.R.N.O. No.38
2456154.4831	R	sec.	−1374.5	−0.00074	−0.00081	0.00072	B.R.N.O. No.38
2456179.3608		sec.	−1283.5	−0.00351	−0.00355	−0.00198	IBVS No. 6070
2456202.8746	V	sec.	−1197.5	−0.00312	−0.00312	−0.00153	IBVS No. 6042
2456209.16515	N	sec.	−1174.5	−0.00104	−0.00103	0.00055	The paper
2456214.21991	N	prim.	−1156	−0.00440	−0.00439	−0.00278	The paper
2456220.23745	BVR_cI_c	prim.	−1134	−0.00192	−0.00190	−0.00029	The paper
2456220.3755		sec.	−1133.5	−0.00057	−0.00055	0.00104	IBVS No. 6070
2456220.37568	BVR_cI_c	sec.	−1133.5	−0.00039	−0.00037	0.00122	The paper
2456222.2889		sec.	−1126.5	−0.00106	−0.00103	0.00057	IBVS No. 6070
2456222.4247		prim.	−1126	−0.00196	−0.00194	−0.00033	IBVS No. 6070
2456523.31519	VR_cI_c	sec.	−25.5	−0.00112	−0.00058	0.00074	The paper
2456530.2867	VR_cI_c	prim.	0	−0.00161	−0.00106	0.00024	The paper

4 Orbital period analysis

4.1 V1107 Cas

Data of times of minima for this contact binary from 2004 to 2013 were collected. All of these 88 times of minima are CCD data, and are listed in table 3, which were used to correct the period with the ephemeris (HJD) 2456530.2867 (To) + $0.^{d}273406(P_0) \times E$, where T_0 is one of our minimum value, and P_0 was obtained from GCVS (N. N. Samus et al. 2009).[5] The new linear ephemeris is

$$\mathrm{Min.\,I\,(HJD)} = 2456530.2883(\pm 0.0003) + 0\overset{d}{.}27341177(\pm 0.00000006) \times E. \quad (1)$$

[5] Samus, N. N., et al. 2009, General Catalogue of Variable Stars, VizieR Online Data Catalog, B/gcvs ⟨http://cdsarc.u-strasbg.fr/viz-bin/Cat?B/gcvs⟩.

Because the $(O-C)$ diagram derived from this formula shows a long-term decreasing tendency, we at first used a parabola term to fit this $(O-C)$ diagram. However, we found that the residuals of this fitting still showed a cyclical variation. Finally, we used a quadratic change superimposed upon a cyclical change to fit the $(O-C)$ diagram, yielding a fitting of

$$\begin{aligned}\mathrm{Min.\,I\,(HJD)} = {} & 2456530.2878(\pm 0.0006) \\ & + 0\overset{d}{.}27341123(\pm 0.00000024) \times E \\ & - 5.69(\pm 2.06) \times 10^{-11} \times E^2 \\ & + 0.0016(\pm 0.0001)\sin(0\overset{\circ}{.}040E - 53\overset{\circ}{.}6).\end{aligned} \quad (2)$$

The resultant $(O-C)$ and $(O-C)_1$ diagrams are also shown in figures 4 and 5, as the solid line represents. That

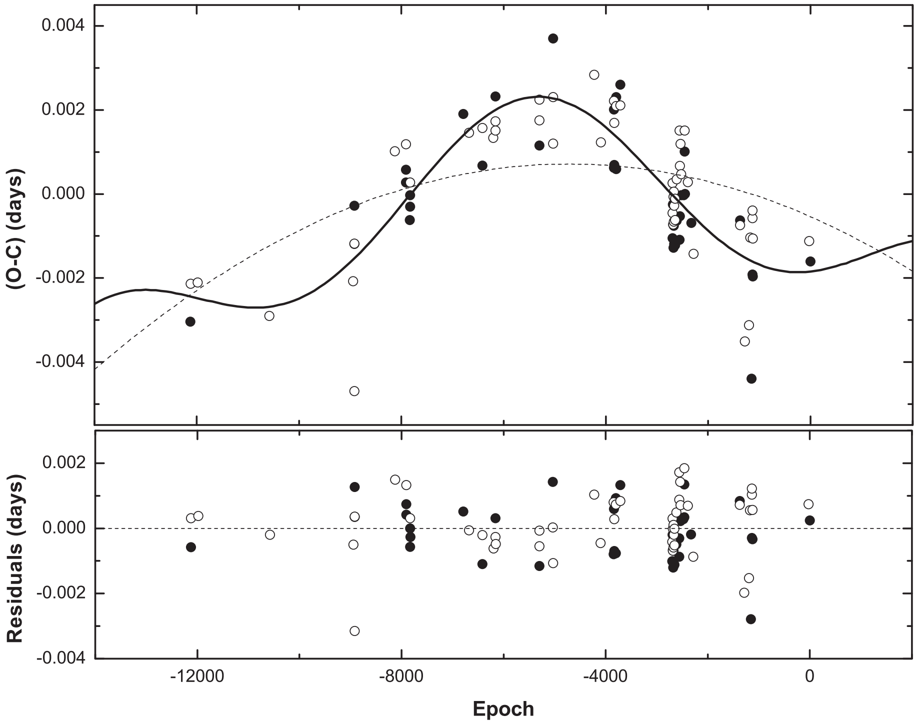

Fig. 4. $(O - C)$ diagram of V1107 Cas formed by all available measurements. The $(O - C)$ values were computed by using a newly determined linear ephemeris, equation (1). The solid circles refer to the primary minima, and the open ones to the secondary minima; the solid line represents a long-term decrease variation, equation (2). The residuals derived from equation (2) are displayed in the lower panel.

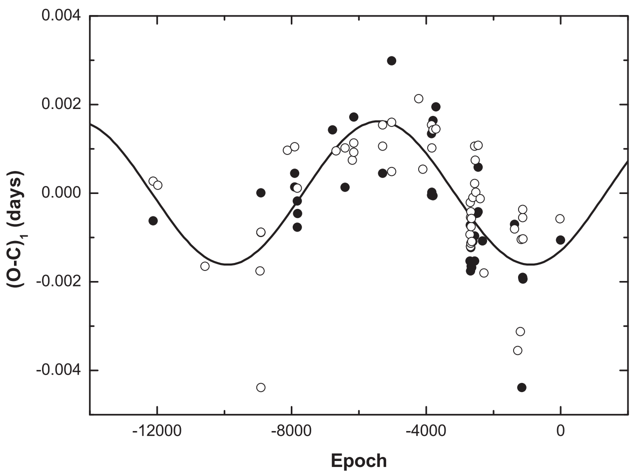

Fig. 5. $(O - C)_1$ diagram of V1107 Cas. The symbols are the same as those in figure 4.

fitting gives a long-term decrease [$dP/dt = -1.52(\pm 0.55) \times 10^{-7}$ d yr^{-1}] with a clear period oscillation [$A_3 = 0\overset{\mathrm{d}}{.}0016$, $T_3 = 6.74$ yr; T_3 was computed by equation (9)]. The residuals are plotted at the bottom of figure 4.

The period decrease should be due to mass transfer from the more-massive component to the less-massive one. If this mass transfer is conservative, we can estimate the mass-transfer rate by using a well-known equation (Tout & Hall 1991), with the absolute parameters derived by the present paper. The formula is

$$\frac{\dot{P}}{P} = 3\frac{\dot{M}_2}{M_2}\left(\frac{M_2}{M_1} - 1\right), \tag{3}$$

so the mass-transfer rate is estimated to be, $dM_2/dt = -1.61(\pm 0.63) \times 10^{-7} M_\odot\,\mathrm{yr}^{-1}$. The negative sign implies that the more-massive component is losing matter. The time-scale of mass transfer is $\tau \sim M_2/\mid \dot{M}_2 \mid \sim 4.3(\pm 1.7) \times 10^6$ yr, which is far greater than the thermal time scale ($t_{\mathrm{th}} = 2 \times 10^7 M^2 R^{-1} L^{-1}$ yr, where M, R, and L are all in solar units) of the more-massive component [$t_{\mathrm{th}} = 7.4(\pm 4.6) \times 10^7$ yr]. The mass-transfer rate is so great that the less-massive component accepting the matter cannot redistribute it in time, so that the temperature of the less-massive component rises. That is why the temperature difference between the two components is as high as 543 K.

As shown in figures 4 and 5, both the primary and the secondary times of light minimum light follow the same general trend of an $(O - C)$ variation, indicating that the $(O - C)$ oscillation cannot be explained as apsidal motion. Because V1107 Cas contains later-type components, its alternate period change can be interpreted in term of the mechanism of magnetic activity (e.g., Applegate 1992; Lanza et al. 1998). However, according exhaustive statistical work, Liao and Qian (2010) pointed out that the

Table 4. Masses and orbital radii of the assumed third bodies in AX Cas and V1107 Cas.

Parameters	AX Cas $M_1 = 2.0 M_\odot$	AX Cas $M_1 = 0.9 M_\odot$	V1107 Cas	Units
A_3	0.0084(±0.0044)	0.0084(±0.0044)	0.0016(±0.0001)	d
T_3	13.8(±0.3)	13.8(±0.3)	6.74(±0.24)	yr
e'	0.2533(±0.1167)	0.2533(±0.1167)	0(assumed)	—
w'	87°.8(±4.6)	87°.8(±4.6)	—	°
$a'_{12} \sin i'$	1.45(±0.19)	1.45(±0.19)	0.28(±0.10)	au
$f(m)$	$1.61(\pm0.94) \times 10^{-2}$	$1.61(\pm0.94) \times 10^{-2}$	$4.68(\pm0.9) \times 10^{-4}$	$M_\odot$
m_3 ($i' = 90°$)	0.509(±0.028)	0.319(±0.028)	0.086(±0.018)	$M_\odot$
m_3 ($i' = 70°$)	0.546(±0.029)	0.344(±0.029)	0.092(±0.019)	$M_\odot$
m_3 ($i' = 50°$)	0.692(±0.046)	0.440(±0.046)	0.114(±0.066)	$M_\odot$
m_3 ($i' = 30°$)	1.169(±0.211)	0.766(±0.211)	0.182(±0.011)	$M_\odot$
m_3 ($i' = 10°$)	5.975(±0.540)	4.698(±0.540)	0.646(±0.040)	$M_\odot$
a_3 ($i' = 90°$)	8.2(±1.5)	6.5(±1.5)	3.8(±0.5)	au
a_3 ($i' = 70°$)	8.2(±1.3)	6.5(±1.3)	3.8(±0.5)	au
a_3 ($i' = 50°$)	8.3(±1.8)	6.6(±1.8)	3.8(±0.8)	au
a_3 ($i' = 30°$)	8.8(±2.5)	7.1(±2.5)	3.9(±0.8)	au
a_3 ($i' = 10°$)	11.7(±3.2)	10.3(±3.2)	4.3(±1.1)	au

most plausible explanation for the cyclic period changes is the light travel time effect (LTTE) through the presence of a third body. By assuming a circular orbit, expressed by the equation

$$f(m) = \frac{4\pi^2}{GT_3^2} \times (a'_{12} \sin i')^3, \quad (4)$$

(where $a'_{12} \sin i' = A_3 \times c$ and c is the speed of light), the mass function for the assumed tertiary component is computed. The following equation is then used

$$f(m) = \frac{(m_3 \sin i')^3}{(M_1 + M_2 + m_3)^2} \quad (5)$$

By taking into account the physical parameters, we obtained (section 3) the masses and the orbital radii of the third companion by computation. The values for several different orbital inclinations (i') are given in table 4. As shown in this table, the assumed tertiary component is invisible unless the orbital inclination, i', is very small ($i' < 10°$). If the tertiary companion is coplanar to the eclipsing pair (i.e., with the same inclination as the eclipsing binary), its mass should be $m_3 = 0.097 \pm 0.019 M_\odot$, which is too small to be detected.

4.2 AX Cas

AX Cas has been monitored for a long time since 1937. We collected all of 60 times of minimum light, consisting of 14 visual and photographic data and 46 photoelectric and CCD ones (table 5). Because the visual and photographic data showed a very large scatter, we only used the 46 CCD data points to correct the period with the ephemeris, 2456220.22457 + $0^{\rm d}.600367560 \times E$, where T_0 is one of our minimum value, and P_0 was obtained from Alfonso-Garzón et al. (2012). The new linear ephemeris is

$$\begin{aligned} \text{Min. I (HJD)} = & 2456220.2205(\pm0.0010) \\ & + 0^{\rm d}.60037157(\pm0.00000031) \times E. \end{aligned} \quad (6)$$

We then used this linear ephemeris to calculate the $(O - C)$ values for all 60 data points, yielding an $(O - C)$ diagram, as shown in figure 6, where the solid cycles refer to the photoelectric or CCD primary minima, and the open ones refer to the photoelectric or CCD secondary minima; the crosses denote the visual or photographic minima, meanwhile; the solid line represents an eccentric ephemeris variation. A long-term period variation can be very clearly seen in figure 6. A parabola formula was used to fit this $(O - C)$ diagram, yielding a fitting of

$$\begin{aligned} \text{Min. I (HJD)} = & 2456220.2204(\pm0.0004) \\ & + 0^{\rm d}.600371245(\pm0.00000003) \times E \\ & - 5.462(\pm0.007) \times 10^{-11} \times E^2. \end{aligned} \quad (7)$$

By using the quadratic term in this equation, a possible secular period increase rate is determined as being $dP/dt = -6.646(\pm0.009) \times 10^{-8}\,{\rm d\,yr^{-1}}$. However, we found that the residuals of the $(O - C)$ still showed a cyclic variation. Hence, we calculated the $(O - C)_1$ values for all 60 data first using equation (7), then performing an eccentric orbit fitting to simulate the photoelectric and CCD $(O - C)_1$

Table 5. Times of light minima for AX Cas.

JD (Hel.)	Method	Min.	Epoch	$(O - C)$ (d)	$(O - C)_1$ (d)	Residuals (d)	Reference
2428626.43100	photog.	prim.	−45961	−0.11177	−0.01116		(O − C) gate way*
2428635.45000	photog.	prim.	−45946	−0.09834	0.00219		(O − C) gate way*
2429114.53800	photog.	prim.	−45148	−0.10686	−0.01003		(O − C) gate way*
2429162.58600	photog.	prim.	−45068	−0.08858	0.00787		(O − C) gate way*
2429165.59700	photog.	prim.	−45063	−0.07944	0.01699		(O − C) gate way*
2429883.60800	photog.	prim.	−43867	−0.11284	−0.02182		(O − C) gate way*
2429903.46200	photog.	prim.	−43834	−0.07110	0.01976		(O − C) gate way*
2429932.26400	photog.	prim.	−43786	−0.08694	0.00371		(O − C) gate way*
2430100.36500	photog.	prim.	−43506	−0.08998	−0.00056		(O − C) gate way*
2430462.39200	photog.	prim.	−42903	−0.08703	−0.00027		(O − C) gate way*
2430839.43100	photog.	prim.	−42275	−0.08138	0.00266		(O − C) gate way*
2431001.52600	photog.	prim.	−42005	−0.08670	−0.00381		(O − C) gate way*
2431145.60900	photog.	prim.	−41765	−0.09288	−0.01101		(O − C) gate way*
2448562.47700	vis	prim.	−12755	−0.00412	0.00076		BAV No. 60
2450752.62980	CCD	prim.	−9107	−0.00681	−0.00509	−0.00498	BBSAG No. 116
2451336.20300	CCD	prim.	−8135	0.00522	0.00633	−0.00066	(O − C) gate way*
2451430.46300	CCD	prim.	−7978	0.00689	0.00791	0.00006	IBVS No. 5016
2451780.48370	CCD	prim.	−7395	0.01096	0.01168	0.00187	IBVS No. 5296
2452576.57300	CCD	prim.	−6069	0.00756	0.00773	0.00020	IBVS No. 5378
2452992.62680	CCD	prim.	−5376	0.00386	0.00383	−0.00063	IBVS No. 5502
2453215.36440	CCD	prim.	−5005	0.00361	0.00348	0.00074	IBVS No. 5731
2453254.38610	CCD	prim.	−4940	0.00116	0.00102	−0.00141	IBVS No. 5657
2454085.29620	CCD	prim.	−3556	−0.00300	−0.00332	0.00061	IBVS No. 5657
2454092.49970	CCD	prim.	−3544	−0.00396	−0.00428	−0.00029	IBVS No. 5657
2454097.30370	CCD	prim.	−3536	−0.00293	−0.00325	0.00076	IBVS No. 5781
2454367.46880	CCD	prim.	−3086	−0.00503	−0.00537	0.00040	IBVS No. 5830
2454388.48350	CCD	prim.	−3051	−0.00334	−0.00368	0.00220	IBVS No. 5830
2454390.28310	CCD	prim.	−3048	−0.00485	−0.00519	0.00070	IBVS No. 5830
2454405.29190	CCD	prim.	−3023	−0.00534	−0.00568	0.00029	IBVS No. 5889
2454704.87190	CCD	prim.	−2524	−0.01076	−0.01109	−0.00397	IBVS No. 5875
2454752.30070	CCD	prim.	−2445	−0.01131	−0.01164	−0.00444	IBVS No. 5889
2454776.31950	CCD	prim.	−2405	−0.00737	−0.00770	−0.00047	IBVS No. 5889
2454847.46690	CCD	sec.	−2286.5	−0.00401	−0.00432	0.00293	IBVS No. 5918
2455154.55560	CCD	prim.	−1775	−0.00536	−0.00562	0.00082	IBVS No. 5941
2455473.35500	CCD	prim.	−1244	−0.00327	−0.00344	0.00052	IBVS No. 6010
2455479.36000	CCD	prim.	−1234	−0.00198	−0.00216	0.00174	IBVS No. 5984
2455482.36010	CCD	prim.	−1229	−0.00374	−0.00391	−0.00003	B.R.N.O. No.37
2455491.36780	CCD	prim.	−1214	−0.00161	−0.00178	0.00200	IBVS No. 5984
2455491.66050	CCD	sec.	−1213.5	−0.00910	−0.00927	−0.00548	IBVS No. 5984
2455514.48530	CCD	sec.	−1175.5	0.00158	0.00141	0.00495	IBVS No. 5984
2455792.45730	CCD	sec.	−712.5	0.00154	0.00147	0.00170	B.R.N.O. No.38
2455794.55580	CCD	prim.	−709	−0.00126	−0.00132	−0.00111	B.R.N.O. No.38
2455797.55730	CCD	prim.	−704	−0.00161	−0.00167	−0.00149	B.R.N.O. No.38
2455799.35880	CCD	prim.	−701	−0.00123	−0.00129	−0.00114	B.R.N.O. No.38
2455802.36020	CCD	prim.	−696	−0.00169	−0.00174	−0.00163	B.R.N.O. No.38
2455805.36250	CCD	prim.	−691	−0.00125	−0.00130	−0.00122	B.R.N.O. No.38
2455820.37150	CCD	prim.	−666	−0.00153	−0.00158	−0.00170	IBVS No. 6026
2455830.28170	CCD	sec.	−649.5	0.00253	0.00248	0.00222	B.R.N.O. No.38
2455831.48280	CCD	sec.	−647.5	0.00289	0.00284	0.00257	B.R.N.O. No.38
2455835.38070	CCD	prim.	−641	−0.00162	−0.00167	−0.00198	IBVS No. 6026
2455838.38330	CCD	prim.	−636	−0.00088	−0.00092	−0.00127	B.R.N.O. No.38
2455858.50250	CCD	sec.	−602.5	0.00587	0.00583	0.00521	IBVS No. 6026
2455875.31200	CCD	sec.	−574.5	0.00497	0.00493	0.00409	B.R.N.O. No.38
2455905.62820	CCD	prim.	−524	0.00240	0.00238	0.00114	IBVS No. 6011
2456154.48730	CCD	sec.	−109.5	0.00749	0.00758	0.00315	B.R.N.O. No.38

Table 5. (Continued)

JD (Hel.)	Method	Min.	Epoch	(O − C) (d)	$(O-C)_1$ (d)	Residuals (d)	Reference
2456179.39980	CCD	prim.	−68	0.00457	0.00468	−0.00004	IBVS No. 6070
2456214.22009	CCD	prim.	−10	0.00331	0.00344	−0.00169	The paper
2456220.22457	CCD	prim.	0	0.00407	0.00420	−0.00100	The paper
2456292.26870	CCD	prim.	120	0.00361	0.00378	−0.00224	JAAVSO No. 42
2456535.42480	CCD	prim.	525	0.00923	0.00954	0.00125	B.R.N.O. No.38

*⟨http://var.astro.cz/ocgate/ocgate.php?star=ax+cas&submit=Submit&lang=en⟩.

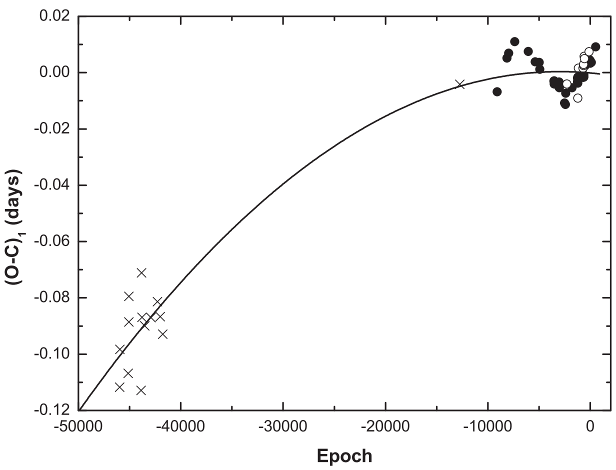

Fig. 6. $(O-C)$ diagram of AX Cas formed by all available measurements. The $(O-C)$ values were computed by using a newly determined linear ephemeris, equation (6). The solid circles refer to the photoelectric or CCD primary minima and the open ones to the photoelectric or CCD secondary minima; the crosses denote visual or photographic minima, while the solid line represents an eccentric ephemeris variation.

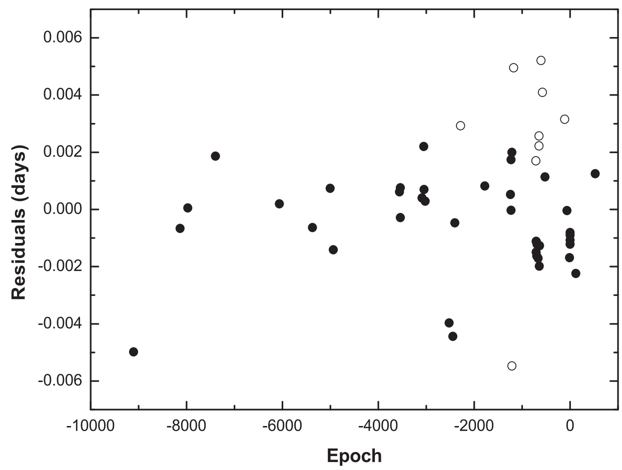

Fig. 8. CCD residuals, equation (8), of $(O-C)_1$ diagram of AX Cas. The symbols are the same as those in figure 4.

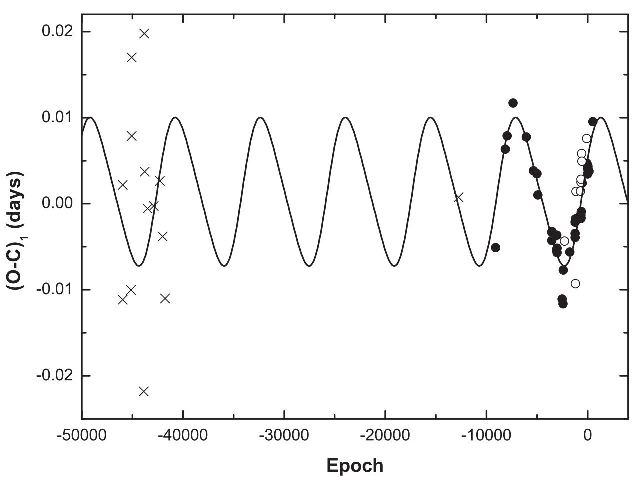

Fig. 7. $(O-C)_1$ diagram of AX Cas determined by equation (7). The symbols are the same as those in figure 4.

values. The result is:

$$
\begin{aligned}
(O-C)_1 = {} & 0.0014(\pm 0.0004) \\
& + 0.0031(\pm 0.0002)\cos 0\overset{\circ}{.}0428E \\
& + 0.0078(\pm 0.0018)\sin 0\overset{\circ}{.}0428E \\
& + 0.0007(\pm 0.0018)\cos 0\overset{\circ}{.}0856E \\
& + 0.0008(\pm 0.0008)\sin 0\overset{\circ}{.}0856E.
\end{aligned} \tag{8}
$$

The corresponding $(O-C)_1$ curve is shown in figure 7, where the symbols are the same as those in figure 6. The corresponding residuals are plotted in figure 8. With the aid of the following relations (Kopal 1978):

$$\omega = 360^\circ P_e/T, \tag{9}$$

$$A_3 = \sqrt{a_1^2 + b_1^2}, \tag{10}$$

$$e' = 2\sqrt{\frac{a_2^2 + b_2^2}{a_1^2 + b_1^2}}, \tag{11}$$

$$w' = \arctan\frac{(b_1^2 - a_1^2)b_2 + 2a_1b_1a_2}{(a_1^2 - b_1^2)a_2 + 2a_1b_1b_2}, \tag{12}$$

the period of the orbital oscillation was determined to be $T_3 = 13.8$ yr with an eccentricity of $e' = 0.2533$; P_e is the ephemeris period ($0^{\rm d}.60037157$); e' is the orbital eccentricity; w' is the longitude of the orbital periastron, and a_1, b_1, a_2, and b_2 are the corresponding fitting coefficients ($a_1 = 0.0031$, $b_1 = 0.0078$, $a_2 = 0.0007$, and $b_2 = 0.0008$). This eccentrical period oscillation may be caused by the light travel-time effect (LTTE) of a tertiary component. Then, by using equations (4) and (5), and taking into account the physical parameters $M_1 = 2.0\,M_\odot$, and $M_2 = 0.45\,M_\odot$ (M. A. Svechnikov & Eh. F. Kuznetsova 1990),[4] the masses and the orbital radii of the third companion were computed. The values for several different orbital inclinations (i') are given in table 4. If the tertiary companion is coplanar to the eclipsing pair (i.e., with the same inclination as the eclipsing binary), its mass should be $m_3 = 0.54 \pm 0.03\,M_\odot$.

However, the primary component of AX Cas may not be as large as $2.0\,M_\odot$. As mentioned in section 1, the temperature of the AX Cas' primary component would be 5600 ± 370 K according to the colors, suggesting that $M_1 = 0.90 \pm 0.16\,M_\odot$, $R_1 = 0.90\,R_\odot$, and $L_1 = 0.719\,L_\odot$. If we agreed with the mass ratio ($q = M_2/M_1 = 0.225$) determined by M. A. Svechnikov and Eh. F. Kuznetsova (1990),[4] we obtain $M_2 = 0.20 \pm 0.04\,M_\odot$. The new set of masses for the components of AX Cas were used to compute the mass of the third body. One can find this new result in table 4. In this case, the mass of the m_3 is $0.34 \pm 0.03\,M_\odot$.

Like V1107 Cas, the mass-transfer time scale, τ, and the thermal time scale, $t_{\rm th}$, of AX Cas were estimated. If $M_1 = 2.0\,M_\odot$, we obtain $\tau \sim 3.01 \times 10^7$ yr and $t_{\rm th} = 1.06 \times 10^7$ yr; however, $M_1 = 0.90\,M_\odot$, we have $\tau \sim 1.35 \times 10^7$ yr and $t_{\rm th} = 2.50 \times 10^7$ yr. This indicates that τ and $t_{\rm th}$ are of the same order.

5 Discussion and conclusions

The $VR_{\rm c}I_{\rm c}$ light-curve solution shows that the mass ratio, q, of V1107 Cas is 1.797 ± 0.006, while the fill-out factor is $15.2\% \pm 1.8\%$. The results suggest that V1107 Cas is a W-type moderate mass-ratio shallow contact binary. [The W-type is a contact binary in which the more massive component is the cooler one. Please see the classification by Binnendijk (1970)]. From the temperature (T_2) of the more massive component, we estimated its mass to be $M_2 = 0.70 \pm 0.03$. The rest physical parameters are obtained by using the LC program of the W–D code (Wilson & Devinney 1971; Wilson 1979, 1990, 1994, 2008; Van Hamme & Wilson 2007). Thus, all of the parameters are: $M_1 = 0.39 \pm 0.01\,M_\odot$, $M_2 = 0.70 \pm 0.03\,M_\odot$, $R_1 = 0.52 \pm 0.10R_\odot$, $R_2 = 0.68 \pm 0.12R_\odot$, $L_1 = 0.178 \pm 0.108\,L_\odot$, and $L_2 = 0.196 \pm 0.116\,L_\odot$, where the errors mainly come from the uncertainties in the temperatures of the components. Someone may ask, why you did not use the higher temperature (T_1) of 5200 K to estimate M_1. We can explain this. The temperature of the less-massive component is affected by the more-massive one because of the mass transfer. The material flow heats the less-massive component so that it is much hotter than it would be ordinarily. Such an affected temperature is not suitable for estimating the mass value.

Based on all of the available eclipse times, the period variations of V1107 Cas and AX Cas were investigated. All of them show long-term period decreases of $dP/dt = -1.52(\pm 0.55) \times 10^{-7}\,{\rm d\,yr^{-1}}$ for V1107 Cas and $dP/dt = -6.646(\pm 0.009) \times 10^{-8}\,{\rm d\,yr^{-1}}$ for AX Cas. Besides the long-term period decrease, their periods both indicate cyclic oscillations, with period T_3 of 6.74 years for V1107 Cas and that of 13.8 years for AX Cas. Especially, the oscillation of AX Cas' period is an eccentric one with an e' of 0.2533. The long-term period decreases can be explained as being mass transfer from the more-massive component to the less-massive one, while the cyclic period oscillations can be interpreted as being the light travel-time effect (LTTE) caused by a tertiary companion. The masses and distance to the center binary are listed in table 4.

Based on the coplanar assumption, the m_3 in V1107 Cas system should be $0.097 \pm 0.019\,M_\odot$, while in the AX Cas system it should be $0.34 \pm 0.03\,M_\odot$. A main-sequence star with $0.097 \pm 0.019\,M_\odot$ should be of the M7 type (Cox 2000). The luminosity of M5 is $0.001\,L_\odot$, so the third body in V1107 Cas must be fainter than that. We can safely assume l_3 is $0.0005\,L_\odot$. Such an l_3 is only a 0.13% contribution to the system, which agrees with the 0.16% reduced from the DC program.

Samec and his colleagues have studied several precontact binary systems (i.e., V2421 Cyg, Samec et al. 2014; ZZ Eri, Samec et al. 2015a; V1001 Cas, Samec et al. 2015b). Compared with their work, we believe that AX Cas is also a precontact binary, like V2421 Cyg (Samec et al. 2014). This is also supported by a decreased period rate. Thus, AX Cas is a precontact binary, while V1107 Cas is a shallow contact binary; they have adjoining evolutional stages. That makes the situation much more significance than if they are just in the same field.

Acknowledgement

This work is partly supported by Chinese Natural Science Foundation (Nos. 11403095, 11133007, and 11325315), by the Strategic Priority Research Program "The Emergence of Cosmological Structures" of the Chinese Academy of Sciences, Grant No. XDB09010202, by the Yunnan Natural Science Foundation (2014FB187), and by Youth Innovation Promotion Association CAS.

New observations of the systems were obtained with the 85 cm telescope at Xinglong observation base, and with the 1 m and 60 cm telescope at Yunnan Observatories (YNOs). We thank the person who processed the data.

Especially, we are grateful to Dr. Danny Faulkner, who has offered much help to improve the paper.

References

Alfonso-Garzón, J., Domingo, A., Mas-Hesse, J. M., & Giménez, A. 2012, A&A, 548, A79
Applegate, J. H. 1992, ApJ, 385, 621
Beljawsky, S. 1931, Astron. Nachr., 243, 115
Binnendijk, L. 1970, Vistas Astron., 12, 217
Claret, A., & Gimenez, A. 1990, A&A, 230, 412
Cox, A. N. ed. 2000, Allen's Astrophysical Quantities, 4th ed. (New York: Springer)
Hoffman, D. I., Harrison, T. E., & McNamara, B. J. 2009, AJ, 138, 466
Kopal, Z. 1978, Dynamics of Close Binary Systems (Dordrecht: D. Reidel Publishing Co.)
Lanza, A. F., Rodono, M., & Rosner, R. 1998, MNRAS, 296, 893
Liao, W.-P., & Qian, S.-B. 2010, MNRAS, 405, 1930
Lucy, L. B. 1967, Z. Astrophysik 65, 89
Ruciński, S. M. 1969, Acta Astron., 19, 245
Samec, R. G., Carrigan, B. J., Gray, J. D., French, J. A., McDermith, R. J., & Padgen, E. E. 1998, AJ, 116, 895
Samec, R. G., Clark, J. D., Van Hamme, W., & Faulkner, D. R. 2015a, AJ, 149, 48
Samec, R. G., Koenke, S. S., & Faulkner, D. R. 2015b, AJ, 149, 30
Samec, R. G., Shebs, T. S., Faulkner, D. R., Van Hamme, W., & Mathis, R. F. 2014, AJ, 147, 3
Tout, C. A., & Hall, D. S. 1991, MNRAS, 253, 9
Van Hamme, W., & Wilson, R. E. 2007, ApJ, 661, 1129
Wilson, R. E. 1979, ApJ, 234, 1054
Wilson, R. E. 1990, ApJ, 356, 613
Wilson, R. E. 1994, PASP, 106, 921
Wilson, R. E. 2008, ApJ, 672, 575
Wilson, R. E., & Devinney, E. J. 1971, ApJ, 166, 605
Worthey, G., & Lee, H.-c. 2011, ApJS, 193, 1
Xiang, F.-Y., Xiao, T.-Y., Zhang, B., & Shi, X.-D. 2015a, AJ, 150, 9
Xiang, F.-Y., Xiao, T.-Y., & Yu, Y.-X. 2015b, AJ, 150, 25
Xiang, F.-Y., Yu, Y.-X., & Xiao, T.-Y. 2015c, AJ, 149, 62
Zhou, A.-Y., Jiang, X.-J., Zhang, Y.-P., & Wei, J.-Y. 2009, Res. Astron. Astrophys., 9, 349
Zhu, L., & Qian, S. 2006, MNRAS, 367, 423
Zhu, L., Qian, S.-B., Mikulášek, Z., Zejda, M., Zvěřina, P., & Diethelm, R. 2010, AJ, 140, 215
Zhu, L.-Y., Qian, S.-B., & Yang, Y.-G. 2008, AJ, 136, 337